

VU Research Portal

Heat of solution and site energies of hydrogen in disordered transition-metal alloys

Brouwer, R.C.; Griessen, R.

published in

Physical Review B. Condensed Matter
1989

document version

Publisher's PDF, also known as Version of record

[Link to publication in VU Research Portal](#)

citation for published version (APA)

Brouwer, R. C., & Griessen, R. (1989). Heat of solution and site energies of hydrogen in disordered transition-metal alloys. *Physical Review B. Condensed Matter*, 40(3), 1481-1494.

General rights

Copyright and moral rights for the publications made accessible in the public portal are retained by the authors and/or other copyright owners and it is a condition of accessing publications that users recognise and abide by the legal requirements associated with these rights.

- Users may download and print one copy of any publication from the public portal for the purpose of private study or research.
- You may not further distribute the material or use it for any profit-making activity or commercial gain
- You may freely distribute the URL identifying the publication in the public portal ?

Take down policy

If you believe that this document breaches copyright please contact us providing details, and we will remove access to the work immediately and investigate your claim.

E-mail address:

vuresearchportal.ub@vu.nl

Heat of solution and site energies of hydrogen in disordered transition-metal alloys

R. C. Brouwer and R. Griessen

Natuurkundig Laboratorium, Vrije Universiteit, NL-1081 HV Amsterdam, The Netherlands

(Received 30 December 1988)

Site energies, long-range effective hydrogen-hydrogen interactions, and the enthalpy of solution in transition-metal alloys are calculated by means of an embedded-cluster model. The energy of a hydrogen atom is assumed to be predominantly determined by the first shell of neighboring metal atoms. The semiempirical local band-structure model is used to calculate the energy of the hydrogen atoms in the cluster, taking into account local deviations from the average lattice constant. The increase in the solubility limit and the weak dependence of the enthalpy of solution on hydrogen concentration in disordered alloys are discussed. Calculated site energies and enthalpies of solution in the alloys are compared with experimental data, and good agreement is found. Due to the strong interactions with the nearest-neighbor metal atoms, hydrogen atoms can be used to determine local lattice separations and the extent of short-range order in "disordered" alloys.

I. INTRODUCTION

Hydrogen in metals has been a subject of experimental and theoretical research for many years.¹⁻⁴ Although there is a rather good understanding of the properties of hydrogen in pure (transition) metals, it is presently not possible to calculate accurately the heat of solutions or diffusion coefficients from first principles.⁵⁻⁷ The difficulties encountered for pure metals in first-principles calculations are, of course, even larger for intermetallic compounds and disordered systems, such as alloys.

One is therefore still bound to use semiempirical models. Several models have been proposed in the past and, as discussed by Griessen and Riesterer,⁵ the most accurate model, with the smallest number of fit parameters, is the semiempirical local band-structure model. With this model it is possible to calculate the heat of formation, volume expansion, and site occupation of hydrogen in a large number of pure metals.⁸ In this work we apply the local band-structure model to disordered alloys.

Results on diffusion⁹⁻¹¹ and solution¹² of hydrogen in disordered (transition-) metal alloys indicate that the metal-hydrogen interactions are short ranged and, in a first-order approximation, that only the metal atoms in the first shell determine the energy of the hydrogen atom in a given cluster (or interstitial site). Therefore, in spite of the complexity of disordered alloys, hydrides are well described by means of local-site energies, a Fermi-Dirac distribution, and long-range effective hydrogen-hydrogen interactions.^{10,13} Recently, site energies have been determined for the first time by Feenstra *et al.*¹⁴ in the $\text{Nb}_{1-y}\text{V}_y\text{H}_x$ system, with $0 \leq y \leq 1$, from pressure-composition isotherms. Using these site energies, Brouwer *et al.*¹⁵ showed that diffusion coefficients for hydrogen in the $\text{Nb}_{1-y}\text{V}_y$ alloys could be accurately calculated as a function of temperature and hydrogen concentration over the complete composition (y) range.

Measuring site energies is, considering the large number of compounds and the infinite number of alloys, not a practical method. The calculation of trap (i.e., site) ener-

gies from first principles, however, by several authors led to conflicting predictions and disagreement with experimental data.^{16,17}

The purpose of this paper is to show that the enthalpy of solution in disordered transition-metal alloys can be predicted by a semiempirical embedded-cluster model, based on the local band-structure model, and incorporating a coupling between local-site volumes and the average site volume in the alloy. In Sec. II we describe the method of calculation of the enthalpy of solution of hydrogen in an alloy, and which parameters (site energies, H-H interactions) are needed in the calculations. The embedded-cluster model is presented in Sec. III, and in Sec. IV the effective H-H interaction is calculated, using the semiempirical local band-structure model. To demonstrate the validity of our approach, calculated enthalpies of solution are compared with experimental data, as a function of alloy composition and hydrogen concentration for $\text{Nb}_{1-y}\text{V}_y$, $\text{Ti}_{1-y}\text{V}_y$, $\text{Cr}_{1-y}\text{V}_y$, $\text{Mo}_{1-y}\text{Ti}_y$, $\text{Ta}_{1-y}\text{V}_y$, and $\text{Ta}_{1-y}\text{Nb}_y$ in Sec. V. The results are discussed in Sec. VI.

II. ENTHALPY OF SOLUTION IN DISORDERED ALLOYS

The enthalpy of solution of hydrogen in transition metals at infinite dilution $\Delta\bar{H}_\infty$, defined as $\Delta\bar{H}_\infty = \bar{H}_\infty - \frac{1}{2}\bar{H}_\text{H}$, with \bar{H}_∞ the partial molar enthalpy for hydrogen in metals and \bar{H}_H the partial molar enthalpy for hydrogen gas, was shown to obey the following semiempirical relation:⁸

$$\Delta\bar{H}_\infty = \alpha \Delta E W_d^{1/2} \sum_j R_j^{-4} + \beta, \quad (1)$$

with $\alpha = 18.6$ kJ/mol H ($\text{\AA}^4 \text{eV}^{-3/2}$) and $\beta = -90$ kJ/mol H, and $\Delta E, W_d$ in eV and R_j in \AA . ΔE is a characteristic band-structure energy $\Delta E = E_F - E_S$, with E_F the Fermi energy and E_S essentially the center of the lowest conduction band of the host metal. W_d is the d -band width of the host metal and R_j the distance between

a given hydrogen atom and its neighboring metal atoms. A remarkably good agreement is obtained with the local band-structure model, Eq. (1), between calculated enthalpies of solution and experimental data, for all metals for which experimental band-structure parameters ΔE and W_d are available. Moreover, the site occupancy for hydrogen in fcc (octahedral) and bcc (tetrahedral, see Fig. 1) metals could be predicted by the model.

In a disordered binary alloy $A_{1-y}B_y$, hydrogen atoms occupy sites A_mB_n (Fig. 1) with different energies, i.e., different enthalpies of solution $\Delta\bar{H}_{mn}(y)$. A hydrogen atom occupying an interstitial site A_mB_n has $m+n$ nearest-neighbor metal atoms, n B atoms, and m A atoms. As discussed by several authors, Kirchheim,¹⁰ and Griessen,¹⁸ the distribution of the hydrogen atoms over the interstitial sites is given by a Fermi-Dirac distribution function, as each site can be occupied by, at most, one hydrogen atom, i.e.,

$$c_n = \frac{p_n}{s_n + \exp\{[\Delta\bar{H}_{mn}(y) + f(c) - \mu]/RT\}}, \quad (2)$$

with c_n the hydrogen concentration on sites of type n (c_n is the number of hydrogen atoms on sites of type n , N_n , divided by the total number of interstitial sites, M) and with p_n the fraction of sites of type n in the alloy (p_n is the number of sites of type n , M_n , divided by the total number of sites M ; so $c_n = N_n/M$ and $p_n = M_n/M$ with $c_n/p_n = N_n/M_n$ the partial concentration of hydrogen at sites of type n). The total hydrogen concentration c is given by $c = \sum_n N_n / \sum_n M_n = N/M$, with N the total number of hydrogen atoms. The blocking factor s_n is the number of sites of type n blocked by a hydrogen atom on a site of type n . In the pure metal, s_n depends only on the hydrogen concentration and varies (in a bcc metal) between 7 and 4. However, a good fit to experimental entropies is obtained by taking the limiting value of 4, indicating that at low concentrations the exact value of s in a pure metal is not important.¹⁹ In alloys, s_n depends also

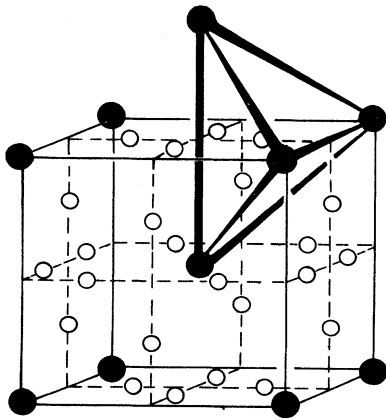


FIG. 1. bcc crystal structure of an alloy $A_{1-y}B_y$. The A and B atoms are randomly distributed among the lattice sites. Hydrogen atoms are occupying the tetrahedral interstitial sites A_mB_n and have four nearest-neighbor metal atoms, $m+n=4$. (●, metal atoms; ○, tetrahedral sites.)

on the type of site n , and on the alloy concentration. If, for example, in an $A_{0.90}B_{0.10}$ alloy a hydrogen atom blocks, on the average, four interstitial sites, the blocking factor for an interstitial on an A_4 site is ~ 4 , but the blocking factor for a hydrogen atom on a B_4 site ~ 1 (the probability of finding another B_4 site next to the interstitial is small). For $c < 0.04$ (24 at. % H), the blocking factor s_n for a hydrogen atom on a tetrahedral interstitial site A_mB_n in a bcc alloy $A_{1-y}B_y$ is approximated by¹⁵

$$s_n = 1 + \frac{3}{4}[m + (n - m)y], \quad (3)$$

assuming that each hydrogen atom blocks, on the average, four interstitial sites.

The long-range effective hydrogen-hydrogen interaction $f(c)$ is assumed to depend only on the total hydrogen concentration c , with $c = \sum_n c_n$.¹⁸ The interaction term $f(c)$ takes into account mean-field electronic and elastic effects due to filling of electronic states at the Fermi energy by the electrons of the hydrogen atoms, and due to long-range H-H interactions via deformation of the lattice.

μ is the chemical potential of the hydrogen atoms in the metal, and R and T have their usual meaning. $\Delta\bar{H}_{mn}(y)$ is the site energy or the local enthalpy of solution depending on the cluster composition (m, n) and on the alloy concentration y .

From expression (2) the total enthalpy of solution $\Delta\bar{H}(y)$ in an alloy $A_{1-y}B_y$ is calculated by using the following relation for the partial molar enthalpy $\bar{H}(y)$,

$$\bar{H}(y) = \left[\frac{\partial(\mu/T)}{\partial(1/T)} \right]_{c,p}, \quad (4)$$

which results in¹³

$$\Delta\bar{H}(y) = f(c) + \frac{\sum_n \Delta\bar{H}_{mn}(y)c_n[1 - (s_n/p_n)c_n]}{\sum_n c_n[1 - (s_n/p_n)c_n]}. \quad (5)$$

In order to be able to calculate the enthalpy of solution in the alloy $\Delta\bar{H}(y)$, the effective H-H interaction $f(c)$ and the site energies $\Delta\bar{H}_{mn}(y)$ have to be determined first.

III. SITE ENERGY

In an alloy $A_{1-y}B_y$ with clusters A_mB_n , the site energy of a hydrogen atom depends strongly on the chemical type of the surrounding atoms, and on the local lattice constants. In Fig. 2 a two-dimensional average lattice, with average lattice constant \bar{a} , is schematically drawn. Metal B has a larger lattice constant than metal A, and the average lattice constant \bar{a} is assumed to interpolate (Vegard's law) between the lattice constants of the two metals. The local B-B (A-A) separation a_{BB} (a_{AA}) in the alloy is, however, somewhat larger (smaller) than the average lattice constant \bar{a} . Therefore, the volume of a B_4 site in the alloy $A_{1-y}B_y$ is in between the average site volume and the volume of a B_4 site in pure metal B. In subsection A the enthalpy of solution $\Delta\bar{H}_{mn}$ of hydrogen in a free cluster A_mB_n is calculated by treating the cluster to be a local alloy $A_{1-y}B_y$ with composition

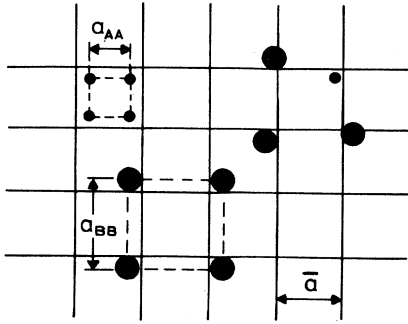


FIG. 2. Schematic representation of an alloy $A_{1-y}B_y$ with an average lattice constant \bar{a} and local lattice constants a_{AA} and a_{BB} . In this two-dimensional lattice, metal B is assumed to have a larger lattice constant than metal A , and the average lattice constant of the alloy is assumed to interpolate linearly between A and B (Vegard's law). The B_4 site has a local lattice constant a_{BB} , larger than \bar{a} but smaller than in pure metal B . The A_4 site is smaller than an average site. A site with three B atoms and one A atom is also schematically drawn in the figure.

$y' = n/(m+n)$. The advantage of this procedure is that the average volume of the alloy $A_{1-y'}B_{y'}$ is exactly equal to the local volume of the cluster A_mB_n . In subsection B the cluster A_mB_n is embedded in the real alloy with composition y , and the enthalpy of solution $\Delta\bar{H}_{mn}(y)$ is calculated, taking into account the local deviations from the average lattice constant.

A. The free cluster

The enthalpy of solution or the site energy of hydrogen in a free cluster $\Delta\bar{H}_{mn}$ with composition $y' = n/(n+m)$ is calculated by means of Eq. (1), if data for the characteristic band-structure parameters ΔE and the d -band width W_d exist. For many compounds and disordered alloys, no data for ΔE and W_d are available. In these cases the procedure proposed by Cyrot and Cyrot-Lackmann²⁰ shall be used for transition-metal alloys, to calculate ΔE and W_d from the data of the pure metals. The various steps in this procedure are schematically indicated in Fig. 3, for an alloy $A_{1-y'}B_{y'}$ with composition $y' = 0.75$ (A_mB_n , with $n=3$) and d -band widths W_a and W_b for the pure metals a and b .

In the first step the bandwidth W_{mn}^* of the compound A_mB_n is set equal to the weighted average of the bandwidths W_a and W_b ,

$$W_{mn}^* = \frac{mW_a + nW_b}{m+n} \quad (6)$$

Since the number of available Bloch states must be constant, the changed bandwidths and band-structure parameters $\Delta E'_a$ and $\Delta E'_b$ are given by

$$\Delta E'_{a(b)} = \Delta E_{a(b)} \frac{W_{mn}^*}{W_{a(b)}} \quad (7)$$

and result in a change in the density of states,

$$n'_{a(b)} = n_{a(b)} \frac{W_{a(b)}}{W_{mn}^*} \quad (8)$$

with $\Delta E'_{a(b)}$ and $n'_{a(b)}$ the rescaled band-structure parameter and the rescaled density of states for metal A (B). As the centers ϵ_a (ϵ_b) of the d band are assumed to be fixed,

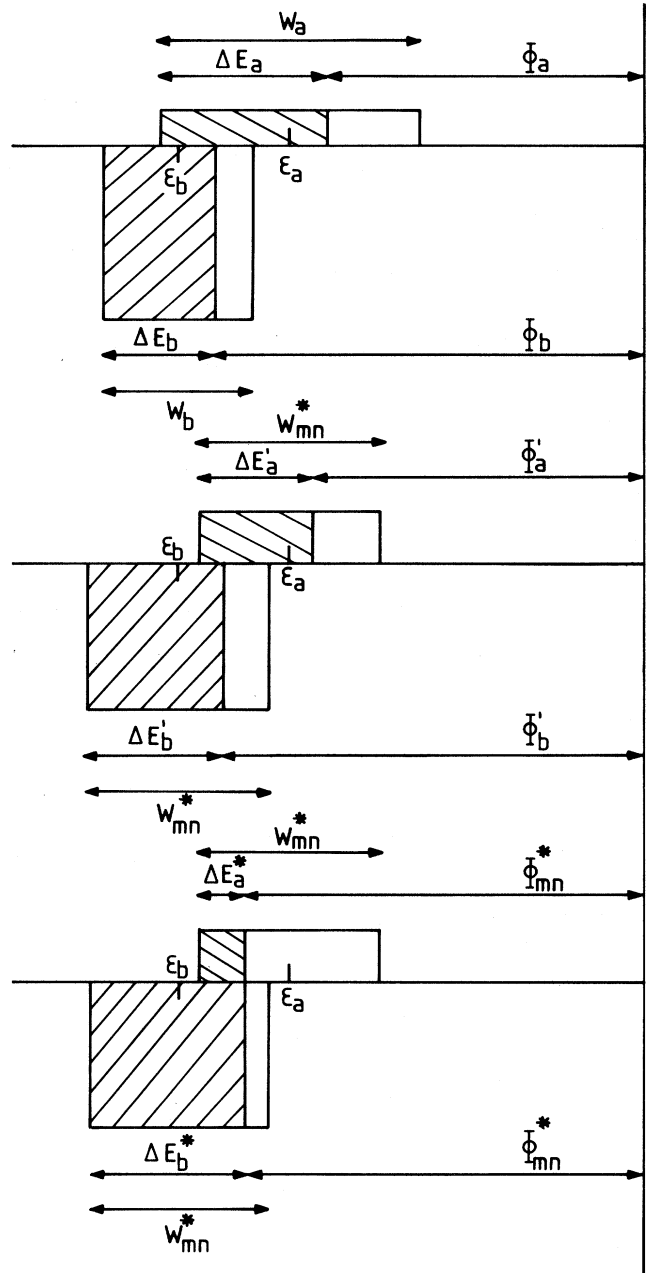


FIG. 3. The construction of the d -band width W_{mn}^* and characteristic band-structure parameter ΔE_{mn}^* for an alloy (or cluster) A_1B_3 . In the first step the bandwidths of the pure metals A and B are rescaled to the weighted average W_{mn}^* , and in the second step electrons are allowed to flow from one band to the other, in order to obtain equal Fermi levels. Along the vertical axis the weighted densities of states are plotted, i.e., nn_A and mn_B (respectively, nn'_A and mn'_B).

the rescaled work functions $\Phi'_{a(b)}$ become

$$\Phi'_{a(b)} = \varepsilon_{a(b)} + \frac{W_{mn}^*}{2} - \Delta E'_{a(b)}. \quad (9)$$

In the second step, electrons are allowed to flow from one band to the other, to obtain equal Fermi levels, and the work function Φ_{mn}^* for the alloy is determined by the condition

$$(\Phi_{mn}^* - \Phi'_a)mn'_a = (\Phi'_b - \Phi_{mn}^*)nn'_b. \quad (10)$$

The rescaled band-structure parameter $\Delta E_{a(b)}^*$ for the metals becomes

$$\Delta E_{a(b)}^* = \Delta E'_{a(b)} + \Phi'_{a(b)} - \Phi_{mn}^*, \quad (11)$$

and the band-structure parameter ΔE_{mn}^* for the alloy is then obtained by means of

$$\Delta E_{mn}^* = \frac{m \Delta E_a^* + n \Delta E_b^*}{m + n}. \quad (12)$$

The enthalpy of solution (or site energy) $\Delta \bar{H}_{mn}$ of hydrogen in the free cluster with composition $A_m B_n$ or in an alloy with composition $y' = n/(n+m)$ can be expressed in analogy to Eq. (1) as

$$\Delta \bar{H}_{mn} = \alpha \Delta E_{mn}^* (W_{mn}^*)^{1/2} \sum_j R_j^{-4} + \beta. \quad (13)$$

The same procedure has been used in Ref. 21 to calculate the average enthalpy of solution of hydrogen in alloys $A_{1-y}B_y$ assuming the existence of only one type of site $A_m B_n$ with composition $y = n/(m+n)$. With this approximation, of course, only a qualitative agreement with experimental data was obtained.

B. The embedded cluster

The site energy $\Delta \bar{H}_{mn}$ for the free cluster considered in the preceding subsection has been calculated for a cluster $A_m B_n$ with local volume

$$\Omega_{mn} = \frac{m\Omega_a + n\Omega_b}{m+n}, \quad (14)$$

with Ω_a and Ω_b the cluster volume of an A_{m+n} or B_{m+n} cluster in the pure metals A and B . The average cluster volume $\bar{\Omega}(y)$ in the real alloy $A_{1-y}B_y$, however, is given by

$$\bar{\Omega}(y) = (1-y)\Omega_a + y\Omega_b. \quad (15)$$

The volume $\Omega_{mn}(y)$ of the embedded cluster $A_m B_n$ in the real alloy $A_{1-y}B_y$, assuming a value between that of the volume of the free cluster, Ω_{mn} , and of the average cluster volume, $\bar{\Omega}(y)$, can be expressed as

$$\Omega_{mn}(y) = (1-D)\bar{\Omega}(y) + D\Omega_{mn}. \quad (16)$$

For $D=0$ the cluster $A_m B_n$ has the average volume and, for $D=1$ the cluster is not influenced by the surrounding lattice (elastically decoupled, free cluster). Froyen and Herring²² calculated the average deviations from the average lattice spacings for random fcc and bcc alloys from the elastic constants c_{11} , c_{12} , and c_{44} . Once the

elastic constants are known, the parameter I_1 of Froyen and Herring can be determined from Fig. 1 in Ref. 22. The parameter D of Eq. (16) is related to I_1 , for bcc alloys and tetrahedral interstitial sites, by the relation (see Appendix)

$$D = 1.58I_1. \quad (17)$$

The parameter D is thus determined from the elastic constants c_{11} , c_{12} , and c_{44} . The volume dependence of the enthalpy of solution, $\Delta \bar{H}(y)$, for hydrogen in an alloy is given by (Sec. IV)

$$\frac{\partial \Delta \bar{H}(y)}{\partial \ln V} = -B\bar{V}_H, \quad (18)$$

with B the bulk modulus of the alloy and \bar{V}_H the molar volume of hydrogen in the alloy. The enthalpy of solution of a hydrogen atom in a cluster $A_m B_n$ in the alloy $A_{1-y}B_y$ is finally given by

$$\Delta \bar{H}_{mn}(y) = \Delta \bar{H}_{mn} - \frac{B\bar{V}_H}{V_m} [\Omega_{mn}(y) - \Omega_{mn}], \quad (19)$$

with V_m the molar volume of the alloy. If no (reliable) experimental data on B , \bar{V}_H and/or V_m , exist, the volume dependence of the band-structure parameter ΔE_{mn}^* and the bandwidth W_{mn}^* can be used to estimate the last term in Eq. (19) as ΔE_{mn}^* and W_{mn}^* vary approximately with volume²³ as $V^{-5/3}$,

$$\Delta E_{mn}^*(y) = \Delta E_{mn}^* \left[\frac{\Omega_{mn}}{\Omega_{mn}(y)} \right]^{5/3}, \quad (20)$$

$$W_{mn}^*(y) = W_{mn}^* \left[\frac{\Omega_{mn}}{\Omega_{mn}(y)} \right]^{5/3}. \quad (21)$$

IV. EFFECTIVE HYDROGEN-HYDROGEN INTERACTION

The effective hydrogen-hydrogen interaction $f(c)$ consists of an electronic and elastic part.²⁴ The electronic interaction is mainly due to a filling of the electronic states at the Fermi level of the metal. The elastic effects are due to long-range deformations of the lattice by the hydrogen atoms. The elastic deformations result in an attractive interaction because hydrogen atoms are dilatation centers which feel the distortion field produced by all other hydrogen atoms, thereby lowering the elastic energy of the system.

Because of the long-range nature of the interactions, $f(c)$ depends primarily on the total hydrogen concentration c . It is assumed that in alloys with various sites $A_m B_n$ the effective H-H interactions do not depend on the chemical composition of a certain site. The validity of this mean-field approach can, of course, only be justified by comparing the predictions of the model with existing data. For some metals (Nb, V, Ta, and Pd) the interaction term $f(c)$ is known in detail and has been derived from pressure-composition isotherms,^{3,25} but for most metals, compounds, and alloys $f(c)$'s have not been determined.

If no experimental data exist for $f(c)$, Eq. (1) should be used to calculate the effective hydrogen-hydrogen interaction. Differentiating with respect to the total concentration c , we find

$$\frac{d \Delta \bar{H}_\infty}{dc} = \left[\frac{\partial \Delta \bar{H}_\infty}{\partial \ln V} \right]_c \left[\frac{\partial \ln V}{\partial c} \right] + \left[\frac{\partial \Delta \bar{H}_\infty}{\partial c} \right]_V. \quad (22)$$

The first term on the right-hand side can be written as²⁴

$$\left[\frac{\partial \Delta \bar{H}_\infty}{\partial \ln V} \right]_c = -B \left[\frac{\partial \Delta \bar{H}_\infty}{\partial p} \right]_c. \quad (23)$$

Using $\partial \bar{H}_H / \partial p = 0$ and $\mu_H = \bar{H}_\infty - T \bar{S}_H$, with \bar{S}_H the partial molar entropy, we obtain

$$\left[\frac{\partial \Delta \bar{H}_\infty}{\partial \ln V} \right]_c = -B \bar{V}_H + BT \frac{\partial \bar{V}_H}{\partial T}, \quad (24)$$

with B the bulk modulus of the hydride and \bar{V}_H the molar volume of hydrogen in the metal. The second term on the right-hand side in Eq. (24) is negligible. The second term on the right-hand side of Eq. (22) combined with Eq. (1) yields

$$\left[\frac{\partial \Delta \bar{H}_\infty}{\partial c} \right]_V = \frac{\alpha \nu}{n(E_F)} W_d^{1/2} \sum_j R_j^{-4}, \quad (25)$$

with $n(E_F)$ the density of states at E_F , and ν the number of electrons added per hydrogen atom at the Fermi level. Except for the early transition metals, $\nu=1$. The total effective hydrogen-hydrogen interaction $f(c)$ obtained from Eqs. (22), (24), and (25) is

$$f(c) = \int_0^c \left[-\frac{B \bar{V}_H^2}{V_m} + \frac{\alpha \nu}{n(E_F)} W_d^{1/2} \sum_j R_j^{-4} \right] dc. \quad (26)$$

The first term in Eq. (26) corresponds to the lowering of the enthalpy due to elastic interactions via deformation of the lattice; the second term is the increase of the enthalpy due to filling of the electronic states at the Fermi level.

In principle, Eq. (26) can be used to calculate $f(c)$ in pure metals and in alloys, if the parameters on the right-hand side are known. However, for alloys not all of the parameters have been determined experimentally. A reasonable estimate can be made by interpolating the unknown parameters between the values for the pure metals, as was clearly demonstrated in the $\text{Nb}_{1-y}\text{V}_y\text{H}_x$ system. A linear interpolation of the effective H-H interaction $f(c)$ for various alloys, between the $f(c)$ of the pure metals, Nb and V, yielded an excellent agreement with experimental enthalpies of solution up to high hydrogen concentrations.²⁵ Even diffusion data, which are very sensitive to the exact value of $f(c)$, could be fitted with an interpolated interaction $f(c)$.¹⁵

The detailed *experimental* determination of the H-H interaction in alloys is difficult. In disordered alloys (as well as in a pure metal) the hydrogen atoms are spread out through the lattice at low hydrogen concentrations.

If the hydrogen concentration is increased in a pure metal, the interaction between the hydrogen atoms increases, thereby decreasing the enthalpy of solution $\Delta \bar{H}_\infty$, until hydride formation (clustering) occurs. Several authors²⁶⁻²⁹ reported an apparent weakening of the H-H interaction on alloying based on the observation of an almost constant $\Delta \bar{H}(y)$ with increasing hydrogen concentration, and/or an increase in the solubility limit. This conclusion is premature, because in an alloy the *distribution* of site energies leads to an increase in $\Delta \bar{H}_\infty$ with increasing hydrogen concentration, thereby compensating the decrease in $\Delta \bar{H}_\infty$ due to the increased H-H interaction. The hydride formation, i.e., clustering of the hydrogen atoms, is prevented by the natural disorder, the *distribution* of sites with different energies *over the sample*. In clustering, the hydrogen atoms would have to occupy sites with high energies.^{30,31}

The existence of sites with different energies makes it difficult to separate the interaction effects $f(c)$ in alloys from the site-filling effects. The long-range nature of the effective hydrogen-hydrogen interaction, and the excellent agreement with experimental data upon assuming an interpolated $f(c)$ in the $\text{Nb}_{1-y}\text{V}_y\text{H}_x$ system, indicate, however, the existence of strong hydrogen-hydrogen interactions in disordered alloys.

V. COMPARISON WITH EXPERIMENTAL DATA

The semiempirical relations derived above can only be justified by a comparison with experimental data. In this section site energies, effective hydrogen-hydrogen interactions, and the enthalpy of solution are calculated as a function of alloy composition and as a function of hydrogen concentration for several ternary transition-metal alloy systems. The calculated enthalpies of solutions are compared with existing experimental data.

The site energies in the alloys are calculated by means of Eqs. (13) and (19), using the parameters for the pure metals listed in Table I. The $\Delta \bar{H}_\infty$ for the pure metals have been established quite accurately; the band-structure data ΔE and W_d are generally less precise. In order to reproduce exactly the experimental values $\Delta \bar{H}_\infty$ for the pure metals by Eq. (1), ΔE and W_d have to be optimized. As can be seen in Table I, the optimized values ΔE^0 and W_d^0 are not much different from the original values. The parameter D is calculated for the pure metals by Eq. (17) from the parameters I_1 in Fig. 1 of Ref. 22. I_1 again is determined from the elastic constants in Refs. 32 and 38. The bulk modulus B , molar volume of hydrogen \bar{V}_H , and molar volume of the alloy V_m in Eq. (19) are interpolated, for the alloys, between the values of these parameters in the pure metals, independent of the type of site $A_m B_n$.

The effective hydrogen-hydrogen interaction $f(c)$ has been determined from experimental data only for a small number of pure metals (Table II). To check the reliability of Eq. (26), $f(c)$ was calculated for these metals. As can be seen in Table II, Eq. (26) provides a reasonable estimate for $f(c)$, at low hydrogen concentrations. In alloys the interaction $f(c)$ is interpolated between the $f(c)$ for the pure metals for reasons discussed in Sec. IV [as far as

TABLE I. Data used in the calculations of the enthalpy of solution in the alloys. From left to right in the columns we have the symbol of the elements, the molar volume V_m , the enthalpy of solution for hydrogen at infinite dilution, $\Delta\bar{H}_\infty$, the band-structure parameter $\Delta E = E_F - E_S$, the d -band width W_d , the density of states at the Fermi level, $n(E_F)$, the work function Φ , the bulk modulus B , the molar volume of hydrogen in the metal \bar{V}_H , the parameter D derived from elastic constants, and the optimized values $\Delta E^0 = \lambda \Delta E$ and $W_d^0 = \lambda W_d$; and λ is determined from $\Delta\bar{H}_\infty = \alpha \Delta E W_d^{1/2} \lambda^{3/2} \sum_j R_j^{-4} + \beta$.

Element	V_m^a (cm ³ /mol)	$\Delta\bar{H}_\infty^b$ (kJ/mol H)	ΔE^c (eV)	W_d^d (eV)	$n(E_F)^e$ (states/atom)	Φ^f (eV)	B^g (kJ/cm ³)	\bar{V}_H^h cm ³ /mol H	D^i	ΔE^0 (eV)	W_d^0 (eV)
V	8.35	-29.5	2.90	6.6	1.64	4.3	157	1.59	0.59	2.69	6.13
Nb	10.8	-35.5	2.90	9.0	1.4	4.3	171	1.88	0.75	2.85	8.84
Ta	10.9	-34	3.40	9.7	1.54	4.25	200	1.69	0.54	3.03	8.42
β -Ti	10.6	-55	2.45	6.6	1.59	4.33	95	1.6	0.76 ^j	2.18	5.89
Cr	7.2	40	4.05	6.8	0.7	4.5	190	1.4	0.48	4.35	7.3
Mo	9.3	40	4.50	9.8	0.65	4.6	273	1.8	0.44	5.01	10.91

^aFrom Ref. 8.

^bFrom Refs. 1, 5, and 33.

^cFrom Refs. 8 and 21.

^dFrom Refs. 8 and 21.

^eFrom Ref. 34.

^fFrom Ref. 35.

^gFrom Ref. 36.

^hFrom Refs. 1 and 37.

ⁱFrom Refs. 22, 32, and 38.

^jExtrapolated from data for Ti_{1-y}V_y alloys in Ref. 32.

they exist, experimental $f(c)$'s for the pure metals were used in the calculation of the enthalpy of solution in the alloys].

All transition-metal alloys discussed in this paper crystallize in the bcc crystal structure. The hydrogen atoms are assumed to occupy the tetrahedral interstitial sites (Fig. 1). The blocking factors s_n are calculated by means of Eq. (3).

Most of the alloys $A_{1-y}B_y$ are treated as ideal solutions and, consequently, the atoms are randomly distributed among the lattice sites. The site fractions p_n are then given by a binomial distribution function

$$p_n = \binom{m+n}{n} (1-y)^m y^n. \quad (27)$$

In two of the alloy systems (Ti_{1-y}V_y, Mo_{1-y}Ti_y) short-range-order effects have been observed.³⁹⁻⁴² In an alloy with short-range order σ , the probability of finding an A atom next to another A atom is defined as^{13,43}

$$p_{AA} = p_A + (1-p_A)\sigma. \quad (28)$$

The related pair probabilities p_{AB} , p_{BB} , and p_{BA} are given by

$$p_{AB} = p_B - p_B\sigma,$$

$$p_{BB} = p_B + (1-p_B)\sigma, \quad (29)$$

$$p_{BA} = p_A - p_A\sigma,$$

with p_{AB} meaning the probability of finding a B atom next to the A atom in the lattice.

For positive σ the A and B atoms form clusters of like atoms. An ideal solution of A and B atoms results for $\sigma \approx 0$. For $\sigma < 0$ the A and B atoms form pairs of unlike atoms, which can result in the formation of ordered compounds for large negative values of σ . The cluster fractions p_n are strongly influenced by the amount of short-range order σ in the alloys. As an exact relation between σ and the cluster fractions cannot be found, two models, a "chain" model and a "cluster" model, which both describe the statistical relation between the number of pairs (i.e., σ) and the number of sites (i.e., p_n), were derived, as a function of the alloy concentration. The derivation of these relations is, however, beyond the scope of this paper and therefore the results will be published elsewhere,³⁹ together with the Monte Carlo calculations. For

TABLE II. Parameters A_i^c and A_i ($i=1,2,3,4$) in kJ/mol H entering the expressions for the calculated effective H-H interaction $f^c(c) = A_1^c c$ and the experimentally determined H-H interaction $f(c) = A_1 c + A_2 c^2 + A_3 c^3 + A_4 c^4$. The concentration c is given by the number of hydrogen atoms per tetrahedral site.

Element	A_1^c (kJ/mol H)	A_1 (kJ/mol H)	A_2 (kJ/mol H)	A_3 (kJ/mol H)	A_4 (kJ/mol H)
V ^a	-202	-222	4.35×10^3	-7.78×10^4	5.55×10^5
Nb ^a	-253	-193	2.10×10^3	-2.36×10^4	1.09×10^5
Ta ^b	-242	-166	2.50×10^3	-3.06×10^4	1.83×10^5
β -Ti ^c	-77	-60			
Cr	-54				
Mo	-330				

^aFrom Ref. 25.

^bFrom Ref. 3.

^cFrom Ref. 33.

$\text{Ti}_{1-y}\text{V}_y$ and $\text{Mo}_{1-y}\text{Ti}_y$, in which systems' short-range-order effects were observed,³⁹⁻⁴² we shall use the chain model for $\sigma < 0$ and the cluster model for $\sigma > 0$ to determine the short-range order in the alloys from the enthalpy of solution, $\Delta\bar{H}(y)$.

The enthalpy of solution is calculated using Eqs. (2) and (5). Experimental enthalpies of solution, $\Delta\bar{H}(y)$, for the alloys discussed in this section are listed in Tables III and IV. The $\Delta\bar{H}(y)$ in the alloys depend on hydrogen concentration and, unlike in the pure metals, also strongly on temperature. At higher temperatures the hydrogen atoms tend to occupy sites with higher energy, thereby increasing the enthalpy of solution. For this reason we listed also the hydrogen concentration and temperature interval for which the data were obtained. In some cases (Table III) various authors reported slightly different values for $\Delta\bar{H}(y)$ in the pure metals. To compare the results, the best literature value of $\Delta\bar{H}(y)$ in the pure metal was taken and all the experimental data were shifted to this common reference point. These corrections are only minor, and the resulting $\Delta\bar{H}(y)$ values for an average hydrogen concentration are given by $\Delta\bar{H}_R(y)$ in Table III.

A. The $\text{Nb}_{1-y}\text{V}_y\text{H}_x$ alloy system

The $\text{Nb}_{1-y}\text{V}_y\text{H}_x$ system is the only alloy system for which site energies were determined experimentally. Feenstra *et al.*¹⁴ determined the site energies from pressure-composition isotherms independently for several alloys. In Fig. 4 the calculated site energies are plotted together with the experimental data for $D=0.55$. We observe that in alloying vanadium with niobium the energy of a V_4 site decreases almost linearly due to the expan-

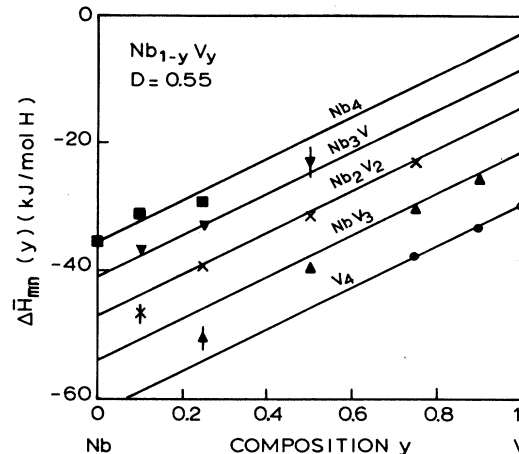


FIG. 4. Site energies $\Delta\bar{H}_{mn}(y)$ for $\text{Nb}_{1-y}\text{V}_y$ alloys as a function of alloy composition. Curves are calculated with the embedded-cluster model. The experimental data for Nb_4 sites (squares), Nb_3V sites (inverted triangles), Nb_2V_2 sites (crosses), NbV_3 sites (triangles), and V_4 sites (solid dots) are obtained from pressure-composition isotherms in Ref. 14. The parameter D was used as a fit parameter. The best fitted, $D=0.55$, is slightly lower than that calculated from elastic constants ($D=0.67$).

sion of the V lattice by the larger Nb atoms. The Nb_4 sites have a smaller volume in the $\text{Nb}_{1-y}\text{V}_y$ alloys than in pure Nb, and therefore the site energy of a Nb_4 site is always higher than in pure Nb. Not all site energies could be determined experimentally from the pressure-composition isotherms. For example, the number of V_4

TABLE III. Experimental enthalpies of solution $\Delta\bar{H}(y)$ measured for a hydrogen concentration c (with c the total number of hydrogen atoms, N , divided by the total number of interstitial sites, M) and temperature T . $\Delta\bar{H}_R(y)$ is the recalculated (experimental) enthalpy of solution for an average hydrogen concentration \bar{c} . To compare results from different authors, the $\Delta\bar{H}(y)$ values for the pure metals were also shifted to the best literature values.

Alloy	$\Delta\bar{H}(y)$ (kJ/mol H)	$10^{-2}c$	T (K)	$\Delta\bar{H}_R(y)$ (kJ/mol H)	$10^{-2}\bar{c}$
V^a	-33.6	0.03-0.17	297-473	-31.4	1
$\text{Ti}_{0.01}\text{V}_{0.99}$	-34.2	0.1-1.7	297-473	-32.1	1
$\text{Ti}_{0.05}\text{V}_{0.95}$	-40.2	0.1-1.7	297-473	-36.6	1
$\text{Ti}_{0.10}\text{V}_{0.90}$	-44.1	0.2-3.3	297-473	-40.5	1
$\text{Ti}_{0.20}\text{V}_{0.80}$	-47.4	0.2-5.0	297-473	-43.8	1
$\text{Ti}_{0.30}\text{V}_{0.70}$	-48.9	0.2-7.0	297-473	-45.3	1
V^a	-33.6	0.03-0.17	297-473	-29.9	0.1
$\text{Cr}_{0.1}\text{V}_{0.9}$	-31.4	0.1	297-473	-27.7	0.1
$\text{Cr}_{0.2}\text{V}_{0.8}$	-29.4	0.1	297-473	-25.7	0.1
$\text{Cr}_{0.3}\text{V}_{0.7}$	-26.6	0.1	297-473	-22.9	0.1
V^b	-31.8	0.4	473-723	-30.6	0.4
$\text{Cr}_{0.02}\text{V}_{0.98}$	-30.9	0.4	473-723	-29.7	0.4
$\text{Cr}_{0.06}\text{V}_{0.94}$	-30.3	0.4	473-723	-29.1	0.4
$\text{Cr}_{0.10}\text{V}_{0.90}$	-28.5	0.4	473-723	-27.3	0.4
$\text{Cr}_{0.15}\text{V}_{0.85}$	-27.3	0.4	473-723	-26.1	0.4
$\text{Cr}_{0.20}\text{V}_{0.80}$	-24.6	0.4	473-723	-23.4	0.4

^aFrom Ref. 27.

^bFrom Ref. 28.

TABLE IV. Experimental enthalpies of solution $\Delta\bar{H}(y)$ measured for an average hydrogen concentration \bar{c} and temperature interval T .

Alloy	$\Delta\bar{H}(y)$ (kJ/mol H)	$10^{-2}\bar{c}$	T (K)
Nb ^a	-35.3	0.1	548-748
Nb _{0.90} V _{0.10}	-38.0	0.1	548-748
Nb _{0.75} V _{0.25}	-40.0	0.1	548-748
Nb _{0.25} V _{0.75}	-34.4	0.1	548-748
Nb _{0.10} V _{0.90}	-31.4	0.1	548-748
V	-29.6	0.1	548-748
Ta _{0.05} V _{0.95} ^b	-32.9	0.83	600-800
Ta _{0.75} V _{0.25} ^b	-38.1	0.83	600-800
Ta _{0.34} V _{0.66} ^c	-37.4	0.83	350-700
Nb _{0.97} Mo _{0.03} ^b	-36.4	0.83	500-700
Ta _{0.7} Nb _{0.3} ^d	-35.0	0.6	600
β -Ti ^e	-54.5	0.3	1100-1200
Mo _{0.21} Ti _{0.79}	-56.1	0.3	1000-1100
Mo _{0.45} Ti _{0.55}	-44.4	0.3	700-1000
Mo _{0.50} Ti _{0.50}	-38.8	0.3	700-1000
Mo _{0.55} Ti _{0.45}	-40.2	0.3	700-1000
Mo _{0.65} Ti _{0.35}	-32.1	0.03	700-1000
Mo ^f	39.7	~0.1	900-1400
Mo _{0.95} Ti _{0.05}	27.2	~0.1	900-1400
Mo _{0.92} Ti _{0.08}	23.0	~0.1	900-1400
Mo _{0.83} Ti _{0.17}	6.3	~0.1	900-1400
Mo _{0.80} Ti _{0.20}	-2.0	~0.1	900-1400
Mo _{0.70} Ti _{0.30}	-14.6	~0.1	900-1400
Mo _{0.63} Ti _{0.37}	-23.0	~0.1	900-1400
Mo _{0.95} Nb _{0.05} ^f	27.2	~0.1	900-1400
Mo _{0.90} Nb _{0.10}	31.4	~0.1	900-1400
Mo _{0.85} Nb _{0.15}	18.8	~0.1	900-1400
Mo _{0.75} Nb _{0.25}	10.5	~0.1	900-1400

^aFrom Ref. 25.

^bFrom Ref. 44.

^cFrom Ref. 29.

^dFrom Ref. 45.

^eFrom Ref. 46.

^fFrom Ref. 47.

sites in a Nb_{0.90}V_{0.10} alloy is so small that their effect on pressure-composition isotherms is negligible.

The parameter D , which determines the local volume of the various sites [Eq. (16)], was used as a fit parameter in calculating the site energies and the enthalpy of solution as a function of the alloy composition and hydrogen concentration (Figs. 5 and 6). A good fit is obtained for $D=0.55$, which is a slightly lower value than the calculated $D=0.67$ from elastic constants, averaged between Nb and V. For small V concentrations the measured site energies (Fig. 4) tend to be somewhat lower for the V_4 and NbV_3 sites than the calculated site energies. In the enthalpy of solution this deviation is almost not observed because the weight of these sites (p_n) is small.

In Fig. 6 the enthalpies of solution for pure V and for a Nb_{0.90}V_{0.10} alloy are plotted as a function of the hydrogen concentration. The curves are obtained from the calculated site energies of Fig. 4 and by interpolating the hydrogen-hydrogen interaction between the experimental data for $f(c)$ in pure V and Nb. An excellent agreement

with the experimental enthalpies of solution is obtained. In the calculation of the concentration dependence of $\Delta\bar{H}(y)$, constant blocking factors $s_n=4$ for all n were used, because at high hydrogen concentrations ($c \geq 0.04$, 24 at. % H) the selective blocking factors s_n [Eq. (3)] are no longer valid. The almost constant $\Delta\bar{H}(y)$ at low hydrogen concentrations in the alloy is due to the cancellation of two effects. With increasing hydrogen concentration, $\Delta\bar{H}(y)$ tends to decrease due to the increasing H-H interactions' $f(c)$. This decrease in $\Delta\bar{H}(y)$, however, is compensated due to a filling of sites with higher energy by the hydrogen atoms with increasing concentration. At higher hydrogen concentrations, $\Delta\bar{H}(y)$ decreases again because H-H interactions becomes dominant (Fig. 6).

B. The Ti_{1-y}V_yH_x system

Nb and V have approximately the same enthalpy of solution for hydrogen and similar electronic structures, but a large difference in lattice parameters. On the other

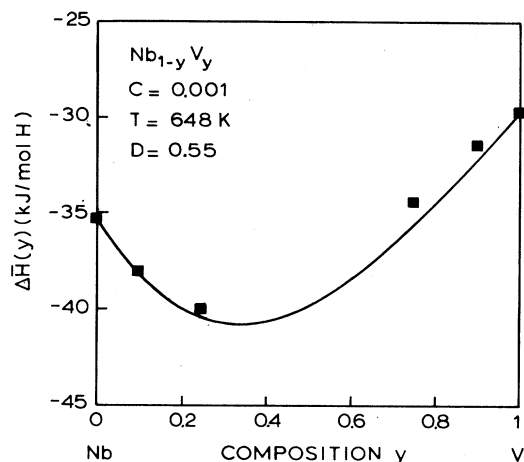


FIG. 5. Enthalpy of solution $\Delta\bar{H}(y)$ in $\text{Nb}_{1-y}\text{V}_y$ alloys calculated as a function of alloy composition at $T=648$ K and for a hydrogen concentration $c=0.001$ (with $c=N/M$, the total number of hydrogen atoms divided by the total number of sites M). The squares are experimental data from Ref. 25.

hand, Ti has a slightly smaller lattice constant than Nb, but is much more favorable for hydrogen absorption, due to a different electronic structure (i.e., a smaller $\Delta E = E_F - E_S$, see Table I). The site energies calculated for the $\text{Ti}_{1-y}\text{V}_y\text{H}_x$ alloy system are displayed in Fig. 7. Now the Ti_4 sites have the lowest energy, and in going from Ti to V the site energy increases due to the decreasing site volumes. Although the volume difference between Ti and V is comparable to that because Nb and V, the slope of the curves for the different sites in the $\text{Ti}_{1-y}\text{V}_y$ system is smaller than in the $\text{Nb}_{1-y}\text{V}_y$ system

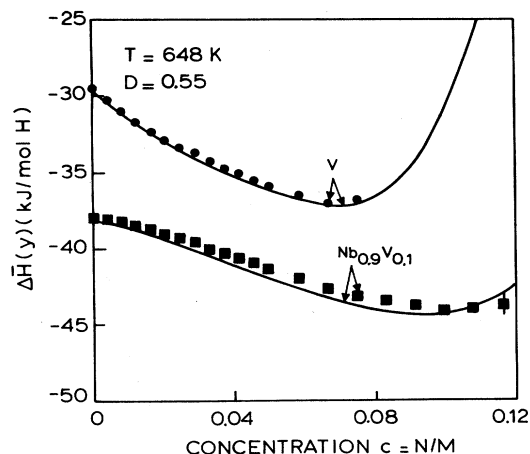


FIG. 6. Enthalpy of solution $\Delta\bar{H}(y)$ as a function of the hydrogen concentration c (with c the number of hydrogen atoms N divided by the total number of sites M) for pure V (circles) and for $\text{Nb}_{0.90}\text{V}_{0.10}$ (squares) at 648 K. The curves are calculated using the calculated site energies of Fig. 4 ($D=0.55$) and a H-H interaction $f(c)$ linearly interpolated between the values for $f(c)$ in pure Nb and V.

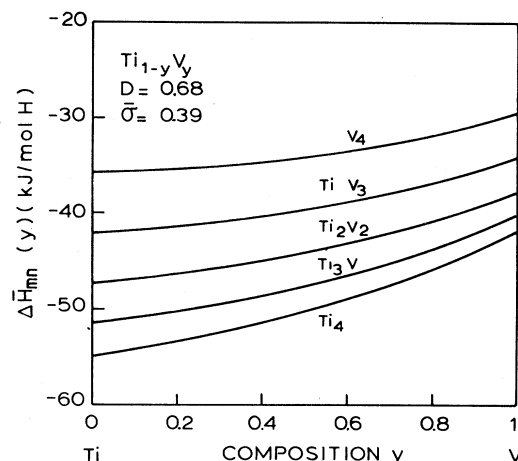


FIG. 7. Site energies $\Delta\bar{H}_{mn}(y)$ for $\text{Ti}_{1-y}\text{V}_y$ alloys as a function of alloy composition, calculated with $D=0.68$ and short-range-order parameter $\bar{\sigma}=0.39$.

(compare Figs. 4 and 7). One reason is that, due to the small bulk modulus in these Ti alloys, a change in site volume results in a relatively small change in $\Delta\bar{H}_{mn}(y)$. The second, and more interesting, reason is that in the $\text{Ti}_{1-y}\text{V}_y$ alloys short-range-order effects are observed.^{39,42} Ti and V atoms tend to form clusters of like atoms. The result is a deviation from the binomial site distribution (i.e., more V_4 and Ti_4 sites and less Ti_2V_2 sites) and an increased tendency for Ti_4 sites to maintain the same volume as in pure Ti, because the local Ti concentration around a Ti_4 cluster is higher than the average Ti concentration in the alloy. The influence of the short-range order on the local volumes is approximated by $D' = D + (1-D)\sigma$, with D calculated from the average elastic constants for the $\text{Ti}_{1-y}\text{V}_y$ alloy system ($D=0.68$).

The only unknown parameter in the calculation of the enthalpy of solution $\Delta\bar{H}(y)$ in Fig. 8 is σ . The short-range-order parameter can now be determined for each alloy independently. As the variation in σ as a function of alloy composition is found to be small, the average value, $\bar{\sigma}$, is given. The solid curve is calculated for $\bar{\sigma}=0.39$ (at 385 K and $c=0.01$, i.e., 6 at. % H) using the site energies in Fig. 7. The dashed curve in Fig. 8 is calculated for an ideal solution of Ti and V in the alloy ($\bar{\sigma}=0$).

C. The $\text{Cr}_{1-y}\text{V}_y\text{H}_x$ alloy system

Unlike Nb and Ti, Cr atoms have a smaller lattice parameter than V, and the Cr metal has a large positive enthalpy of solution (40 kJ/mol H) for hydrogen. In Figs. 9–11 the results are shown for the site energy, the enthalpy of solution as a function of alloy composition, and the enthalpy of solution as a function of hydrogen concentration. The value $D=0.53$ determined from elastic constants was used in the calculations. The V_4 sites are the most favorable sites for hydrogen, and in alloying V with Cr the site energies increase due to the decreasing volume of the lattice. The enthalpy of solution (Fig. 10) increases with Cr content, with an increasing slope, due to the de-

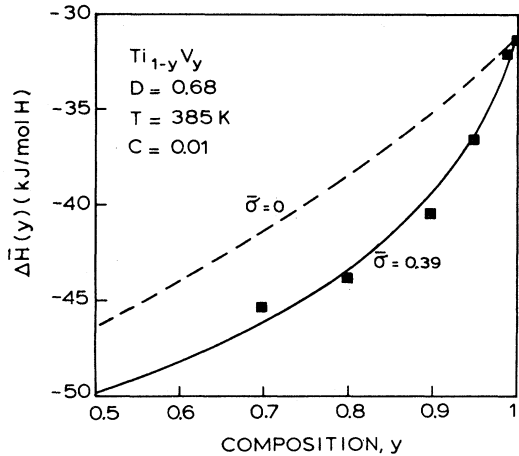


FIG. 8. Enthalpy of solution $\Delta\bar{H}(y)$ for $\text{Ti}_{1-y}\text{V}_y$ alloys as a function of alloy composition at 385 K. The dashed curve is calculated for $D=0.68$ and $\bar{\sigma}=0$, the solid curve for $D=0.68$ and $\bar{\sigma}=0.39$. The squares are experimental data from Ref. 27.

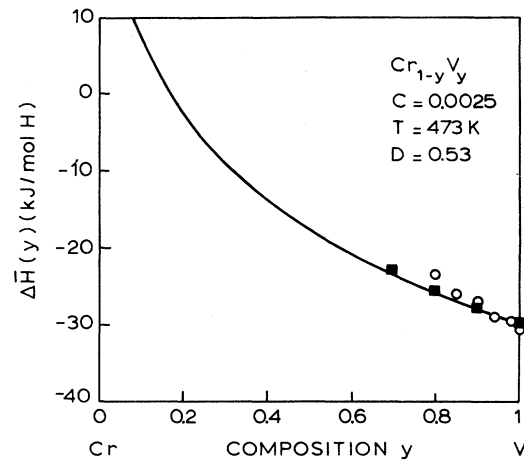


FIG. 10. Enthalpy of solution $\Delta\bar{H}(y)$ for $\text{Cr}_{1-y}\text{V}_y$ alloys as a function of the alloy composition, at $T=473$ K, $c=0.0025$, and $D=0.53$. The curve is calculated using the site energies of Fig. 9, the squares are data from Ref. 27, and the circles are data from Ref. 28.

creasing site volumes combined with site-filling effects.

The hydrogen-concentration dependence for pure V, $\text{Cr}_{0.1}\text{V}_{0.9}$ and $\text{Cr}_{0.15}\text{V}_{0.85}$, Fig. 11, is calculated by using the calculated first-order approximation $f(c)$ for Cr in Table II and the experimental values for $f(c)$ of V. The weakly attractive interaction $f(c) = -54$ kJ/mol H for Cr is due to the small density of states at the Fermi level $n(E_F)$, resulting in strong band-filling effects in the $\text{Cr}_{1-y}\text{V}_y$ system [see Eq. (26)]. A good fit is obtained in Fig. 11 to experimental data for the $\text{Cr}_{0.1}\text{V}_{0.9}$ alloy, while for $\text{Cr}_{0.15}\text{V}_{0.85}$ a deviation is observed at high hydrogen concentrations, probably due to an underestimation of the band-filling effects in $f(c)$.

D. The $\text{Mo}_{1-y}\text{Ti}_y\text{H}_x$ alloy system

The site energies $\Delta\bar{H}_{mn}(y)$, Fig. 12, for the $\text{Mo}_{1-y}\text{Ti}_y$ system have been calculated for $D=0.60$, determined

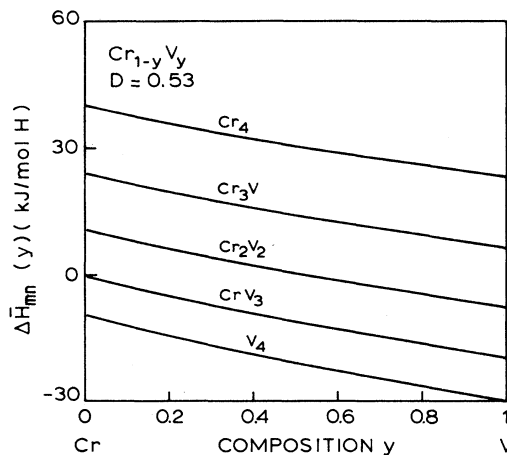


FIG. 9. Site energies $\Delta\bar{H}_{mn}(y)$ for $\text{Cr}_{1-y}\text{V}_y$ alloys as a function of alloy composition, calculated for $D=0.53$.

from elastic constants. Volume effects are relatively unimportant because Mo and Ti have comparable molar volumes, but widely different affinities for hydrogen [$\Delta\bar{H}_\infty(\text{Ti}) = -55$ kJ/mol H, $\Delta\bar{H}_\infty(\text{Mo}) = 40$ kJ/mol H], due to a large difference in the band-structure parameters $\Delta E = E_F - E_S$ and the d -band width W_d . Solubility data for $\text{Mo}_{1-y}\text{Ti}_y$ are plotted in Fig. 13. Experimental data for $\Delta\bar{H}(y)$ exist over the complete composition range. Eguchi *et al.*⁴⁷ (squares) determined $\Delta\bar{H}(y)$ for $0 \leq y \leq 0.37$ at 1200 K and $c \sim 0.001$, and Lynch *et al.*⁴⁶ determined $\Delta\bar{H}(y)$ for $0.35 \leq y \leq 1$ (solid circles) at 850 K and $c = 0.003$. In the $\text{Mo}_{1-y}\text{Ti}_y$ alloys for $0.25 \leq y \leq 0.8$, strong short-range-order effects have been observed by diffusive x-ray scattering.⁴⁰ In contrast to the $\text{Ti}_{1-y}\text{V}_y$

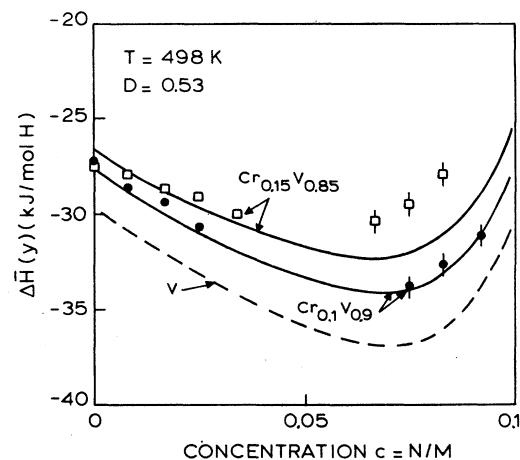


FIG. 11. Enthalpy of solution $\Delta\bar{H}(y)$ for pure V, $\text{Cr}_{0.1}\text{V}_{0.9}$ (circles), and $\text{Cr}_{0.15}\text{V}_{0.85}$ (squares) as a function of the hydrogen concentration at $T=498$ K. The curves are calculated using the site energies in Fig. 9 and a H-H interaction interpolated between the values for $f(c)$ in pure Cr and V ($D=0.53$).

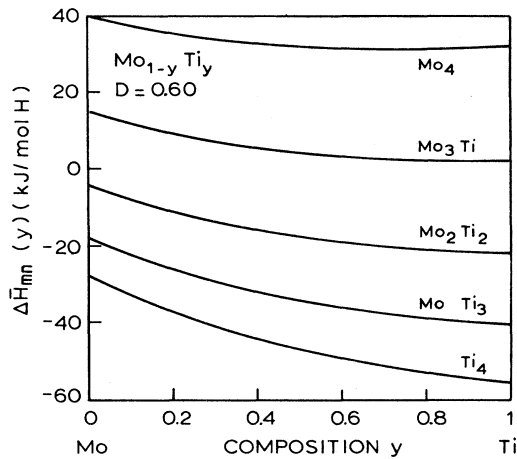


FIG. 12. Site energies $\Delta\bar{H}_{mn}(y)$ for $\text{Mo}_{1-y}\text{Ti}_y$ alloys as a function of alloy composition, for $D=0.60$.

alloys, in $\text{Mo}_{1-y}\text{Ti}_y$ alloys unlike atoms tend to form pairs. Depending on the temperature treatment of the samples $\bar{\sigma}$ values between -0.2 and -0.3 are reported. A negative short-range-order parameter $\bar{\sigma}$ has a strong influence on $\Delta\bar{H}(y)$ at the Mo site of the composition range, because the small number of sites with low energy, the Ti_4 sites, decreases even more. Using the embedded-cluster model with only the short-range-order parameter σ (determining the site distribution p_n) as a fit parameter, the best fit to the data in Fig. 13 is obtained for $\bar{\sigma} = -0.21$, in good agreement with the diffusive x-ray-scattering data. For $\bar{\sigma} = 0$ the $\Delta\bar{H}(y)$ (for $y \lesssim 0.5$) are 15–20 kJ/mol H lower, due to the larger number of Ti_4 sites.

E. The $\text{Ta}_{1-y}\text{V}_y\text{H}_x$ alloy system

This system is much like the $\text{Nb}_{1-y}\text{V}_y\text{H}_x$ alloy system. Ta has a slightly larger molar volume than Nb and al-

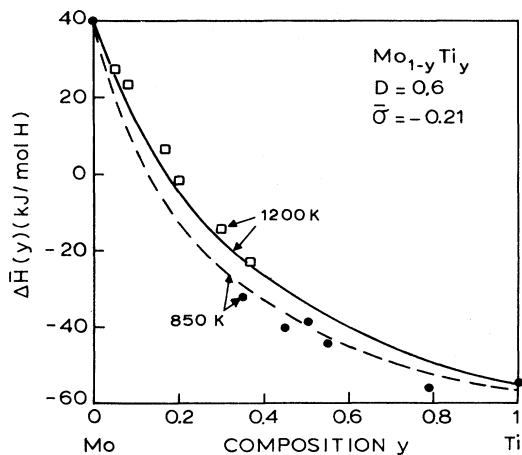


FIG. 13. Enthalpy of solution $\Delta\bar{H}(y)$ for $\text{Mo}_{1-y}\text{Ti}_y$ alloys as a function of alloy composition for $D=0.60$ and a short-range-order parameter of $\bar{\sigma} = -0.21$. The circles are experimental data from Ref. 46 at 850 K, and the squares are data from Ref. 47 at 1200 K.

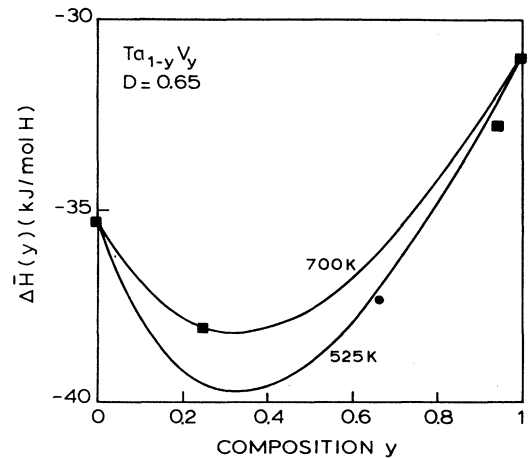


FIG. 14. Enthalpy of solution $\Delta\bar{H}(y)$ for $\text{Ta}_{1-y}\text{V}_y$ alloys at two temperatures, 525 and 700 K, for $c=0.0083$ and $D=0.65$. The curves are calculated from the calculated site energies. Squares are data from Ref. 44 and circle is from Ref. 29.

most the same $\Delta\bar{H}_\infty$. The site energies of the $\text{Ta}_{1-y}\text{V}_y$ system are not displayed here because they resemble those of the $\text{Nb}_{1-y}\text{V}_y$ system in Fig. 4. The best fit to the enthalpies of solution in Fig. 14, at two different temperatures $T=700$ and 525 K for $c=0.0083$ (5 at. % H), is obtained for $D=0.65$, which is slightly higher than the value calculated from elastic constants ($D=0.57$).

F. The $\text{Ta}_{1-y}\text{Nb}_y$ alloy system

Almost no volume effects are expected in this system and Ta and Nb have the same affinities to hydrogen. The interaction parameters $f(c)$ are well established in the pure metals. In Fig. 15 an excellent agreement is obtained between calculated and experimental enthalpies of solution as a function of the hydrogen concentration up

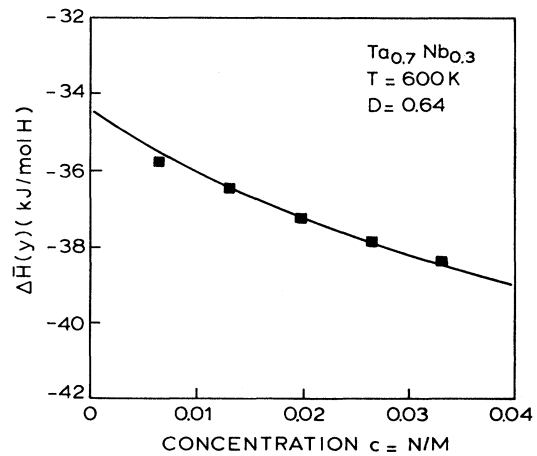


FIG. 15. Enthalpy of solution $\Delta\bar{H}(y)$ for $\text{Ta}_{0.7}\text{Nb}_{0.3}$ at 600 K, as a function of the hydrogen concentration. The curve is calculated from the site energies for $D=0.64$, and using a H-H interaction interpolated between the $f(c)$ of hydrogen in pure Ta and Nb. The squares are data from Ref. 45.

to $c=0.04$ for $D=0.64$ calculated from elastic constants, and a linearly interpolated H-H interaction.

VI. CONCLUSIONS

The embedded-cluster model [Eqs. (13) and (19)] proposed in this paper is of a semiempirical nature. Its use can only be justified by a good agreement between calculated enthalpies of solutions and experimental data. In Fig. 16 we made a comparison between all the calculated and experimental data for the enthalpy of solution in the alloys discussed in this paper. A remarkably good agreement is found.

The embedded-cluster model is based on the assumption that the energy of a hydrogen atom is, in a first approximation, determined by the nearest-neighbor metal atoms. The observation of trapping phenomena⁹⁻¹² and the experimental determination¹⁴ of site energies in the $Nb_{1-y}V_y$ system support this assumption. Sites are assumed to have a volume intermediate between the volume for a free cluster and the average cluster volume in the alloy [Eq. (16)]. The parameter D is a measure of the coupling of a site to the average surrounding lattice. It is related by Eq. (17) to elastic constants. For most alloy systems an averaged value for D , calculated from the elastic constants, results in a good agreement between calculated and experimental enthalpies of solution. In these cases no fit parameter was used at all. Only in the $Nb_{1-y}V_y$ and the $Ta_{1-y}V_y$ alloy system values for D are used, which are slightly lower and slightly higher, respectively, than the D values calculated from elastic constants. This agreement between experimental and calculated values is quite remarkable, considering the strong volume depen-

dence of the enthalpy of solution $\Delta\bar{H}(y)$ [see Eq. (24)]. The importance of having a (simple) semiempirical model is that it provides us with a systematic method to compare quantitatively experimental data of different authors at different alloy concentrations, different hydrogen concentrations, and different temperatures. It provides us also with new insight in the phenomena which can be encountered in these transition-metal-hydrogen alloy systems.

Alloying V with Nb and alloying Nb with V both lead to a decrease in the enthalpy of solution. From Fig. 4 we know that the undersized V forms trap sites in Nb. The decrease in $\Delta\bar{H}(y)$ in alloying V with Nb is not because trap sites are formed, but because the Nb atoms expand the V lattice, thereby decreasing the site energy of the V_4 sites. In the $Mo_{1-y}Ti_y$ and $Cr_{1-y}V_y$ systems the undersized atoms Mo and Cr are very unfavorable for hydrogen and do not form trapping sites. The enthalpy of solution increases in alloying with Mo or Cr due to the contraction of the lattice.

Although the enthalpy of solution decreases in the $Nb_{1-y}V_y$ system and increases in the $Cr_{1-y}V_y$ system, upon alloying with V and with Cr, respectively, the solubility limit (i.e., the hydrogen concentration where hydride formation starts) increases. The observed increase in the solubility limit is thus not simply related to the enthalpy of solution, but is due to the *distribution* of sites with different energy over the lattice.

The effective hydrogen-hydrogen interaction $f(c)$ is shown to be independent of the local disorder, due to its long-range nature. In Figs. 6, 11, and 15 a good agreement with experimental enthalpies of solution is obtained by simply interpolating $f(c)$ for the alloys linearly between the value for $f(c)$ in the pure metals. The *apparent* weakening of the effective hydrogen-hydrogen interactions observed by several authors is due to the *distribution in site energies in the alloys*. Upon increasing the hydrogen concentration, $\Delta\bar{H}(y)$ decreases due to the increasing H-H interactions, but this decrease in $\Delta\bar{H}(y)$ is compensated by an increase in $\Delta\bar{H}(y)$ due to the filling of sites with higher energy.

The site energy $\Delta\bar{H}_{mn}(y)$ of a hydrogen atom depends predominantly on the type of the surrounding atoms, and on the local volume of the cluster. The enthalpy of solution $\Delta\bar{H}(y)$ depends strongly on the site energies $\Delta\bar{H}_{mn}(y)$ and on the number of sites with a certain energy, the site fractions p_n . Therefore, hydrogen atoms can be used as a probe of the local structure of an alloy. From the site energies $\Delta\bar{H}_{mn}(y)$ the local-site volumes, i.e., the local lattice constants (via D), can be calculated.¹⁴ The site fractions are related to the short-range-order parameter σ . Once the relations between σ and the site fractions p_n have been established,³⁹ the amount of short-range order in an alloy can be determined quantitatively. The large short-range order in $Ti_{1-y}V_y$ alloys determined from the enthalpy of solution, $\bar{\sigma}=0.39$, is in agreement with the observation of Ti clusters in diluted $Ti_{1-y}V_y$ alloys by electron-microprobe analysis.⁴² In the related $Ti_{1-y}Nb_y$ system, a short-range order $\bar{\sigma}$ between 0.1 and 0.15 was observed by diffusive x-ray scattering.⁴⁸ The existence of short-range order in the $Ti_{1-y}V_y$ alloys

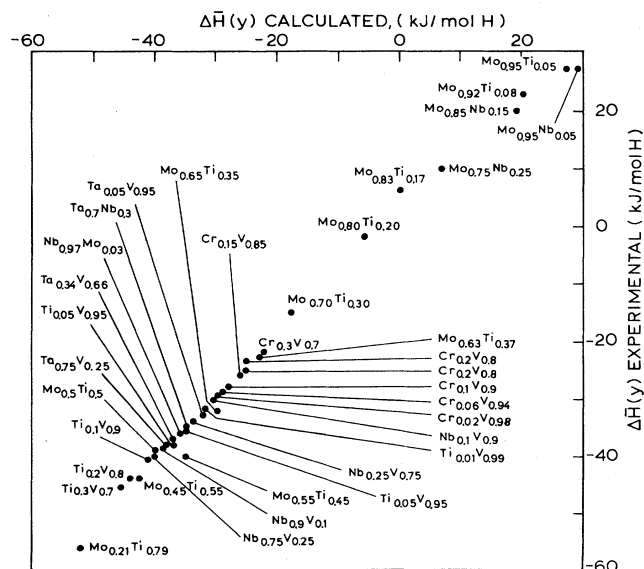


FIG. 16. Comparison of the experimental enthalpies of solution $\Delta\bar{H}(y)$ with the enthalpies of solution calculated by means of the embedded-cluster model for various transition-metal alloys. The temperature interval and hydrogen concentration (\bar{c}) for which $\Delta\bar{H}(y)$ are plotted are found in Tables III and IV.

also explains the widely different activation energies for hydrogen diffusion in these alloys, measured on samples with the same alloy compositions but obtained by different heat treatments. The short-range order $\bar{\sigma}$ in $\text{Ti}_{1-y}\text{V}_y$ alloys determined from diffusion experiments varies between 0.36 and 0.51, in agreement with $\bar{\sigma}$ obtained from the enthalpy of solution.³⁹ For $\text{Mo}_{1-y}\text{Ti}_y$, $\bar{\sigma} = -0.21$ is found from a fit to the enthalpy of solution $\Delta\bar{H}(y)$, in remarkably good agreement with $-0.3 < \bar{\sigma} < -0.2$ reported from diffuse x-ray experiments.⁴⁰ A detailed discussion about short-range-order effects in $\text{Ti}_{1-y}\text{V}_y$ alloys, observed both in solution and diffusion of hydrogen in these alloys, and about the relation between σ and the number of sites (p_n) at a certain energy, will be published elsewhere.

ACKNOWLEDGMENTS

This investigation was part of the research program of the Stichting voor Fundamenteel Onderzoek der Materie (FOM), which is financially supported by the Nederlandse Organisatie voor Zuiver Wetenschappelijk Onderzoek (ZWO).

APPENDIX

Froyen and Herring²² calculated the average change $\langle u \rangle$ from the average near-neighbor separation in random binary alloys. The average change in the A - A , B - B , and A - B near-neighbor separation, for a bcc alloy $A_{1-y}B_y$, is obtained by combining Eqs. (12) and (25) of Ref. 22,

$$\langle u_{AA} \rangle = \frac{\bar{a}}{4} \frac{\partial \ln \bar{\Omega}(y)}{\partial y} (-2y) I_1, \quad (\text{A1a})$$

$$\langle u_{BB} \rangle = \frac{\bar{a}}{4} \frac{\partial \ln \bar{\Omega}(y)}{\partial y} (2-2y) I_1, \quad (\text{A1b})$$

$$\langle u_{AB} \rangle = \frac{\bar{a}}{4} \frac{\partial \ln \bar{\Omega}(y)}{\partial y} (1-2y) I_1, \quad (\text{A1c})$$

with \bar{a} the average lattice constant, $\bar{\Omega}(y)$ the average lattice volume at composition y , and I_1 a parameter which can be determined from the elastic constants c_{11} , c_{12} , and c_{44} in Fig. 1 of Ref. 22. The parameter I_1 determines the local change in the lattice parameter, while the parameter D in Eq. (16) expresses the local volume $\Omega_{mn}(y)$ of a cluster $A_m B_n$ in the average cluster volume $\bar{\Omega}(y)$ and the volume of a free cluster Ω_{mn} . A relation between D and I_1 is simply derived. The (local) relative volume change due to an average change $\langle \partial a \rangle$ in the average lattice constant \bar{a} is given by

$$\frac{(\bar{a} + \langle \partial a \rangle)^3 - \bar{a}^3}{\bar{a}^3} \approx \frac{3\langle \partial a \rangle}{\bar{a}}, \quad (\text{A2})$$

and by

$$\frac{\Omega_{mn}(y) - \bar{\Omega}(y)}{\bar{\Omega}(y)} = D \left[\frac{\Omega_{mn} - \bar{\Omega}(y)}{\bar{\Omega}(y)} \right]. \quad (\text{A3})$$

In Eq. (A3) we can substitute Ω_{mn} by $\bar{\Omega}(n/(m+n))$, and assuming Vegard's law to hold, we obtain

$$D \left[\frac{\bar{\Omega}(n/(m+n)) - \bar{\Omega}(y)}{\bar{\Omega}(y)} \right] = D(n/4-y) \frac{\partial \ln \bar{\Omega}(y)}{\partial y}, \quad (\text{A4})$$

and combining Eqs. (A2) and (A4),

$$D(n/4-y) \frac{\partial \ln \bar{\Omega}(y)}{\partial y} = \frac{3\langle \partial a \rangle}{\bar{a}}. \quad (\text{A5})$$

For a bcc alloy the average change $\langle \partial a \rangle$ in the average lattice parameter, \bar{a} , for a tetrahedral interstitial site is approximately $\langle \partial a \rangle = \frac{1}{6} \sum_{i,j} \langle \partial a_{ij} \rangle$, with the summation over all six bonds of the tetrahedron. In the bcc crystal structure, four bonds are between nearest-neighbor metal atoms with average separation $(\sqrt{3}/2)\bar{a}$. Two bonds are between next-nearest neighbors with bond length \bar{a} . The $\langle \partial a_{ij} \rangle$ are equal to $\langle u_{ij} \rangle$ in Eqs. (A1) for nearest-neighbor metal atoms. Estimating the change in next-nearest-neighbor bonds to be $2\langle u_{ij} \rangle/\sqrt{3}$, the average change in the average lattice parameter for tetrahedral interstitial sites becomes

$$\langle \partial a \rangle = \frac{1}{6} \left[\frac{2}{3} + \frac{1}{3} \left[\frac{2}{\sqrt{3}} \right] \right] \sum_{i,j} \langle \partial u_{ij} \rangle. \quad (\text{A6})$$

If there are k_1 A - A bonds, k_2 B - B bonds, and k_3 A - B bonds in the cluster, then

$$\langle \partial a \rangle = \frac{1}{6} \left[\frac{2}{3} + \frac{1}{3} \left[\frac{2}{\sqrt{3}} \right] \right] \times (k_1 \langle u_{AA} \rangle + k_2 \langle u_{BB} \rangle + k_3 \langle u_{AB} \rangle), \quad (\text{A7})$$

and, in combination with Eqs. (A1) and (A5), we find

$$D(n/4-y) = \frac{I_1}{8} \left[\frac{2}{3} + \frac{1}{3} \left[\frac{2}{\sqrt{3}} \right] \right] \times [-2k_1 y + k_2(2-2y) + k_3(1-2y)]. \quad (\text{A8})$$

The number of B atoms in $A_m B_n$ is related to the number of B - B bonds, k_2 , and the number of A - B bonds, k_3 , by $3n = 2k_2 + k_3$. Using this relation and $k_1 + k_2 + k_3 = 6$, Eq. (A8) is simplified to

$$D = \frac{3}{2} \left[\frac{2}{3} + \frac{1}{3} \left[\frac{2}{\sqrt{3}} \right] \right] I_1 \approx 1.58 I_1, \quad (\text{A9})$$

independent of site type $A_m B_n$ ($n=0,1,\dots,4$) and of alloy composition y . If all bonds in the tetrahedron are equal, then the relation $D = \frac{3}{2} I_1$ is obtained. Now that the relation between I_1 and D is established, D can be calculated from the elastic constants c_{11} , c_{12} , and c_{44} , which determine the value of I_1 (see Fig. 1, Ref. 22).

- ¹*Hydrogen in Metals I and II*, Vols. 28 and 29 of *Topics in Applied Physics*, edited by G. Alefeld and J. Völkl (Springer-Verlag, Berlin, 1978).
- ²J. R. Lacher, Proc. R. Soc. London, Ser. A **161**, 525 (1937).
- ³E. Veleckis and R. K. Edwards, J. Phys. Chem. **73**, 683 (1969).
- ⁴H. Wenzl and J. H. Welter, in *Current Topics in Materials Science 1*, edited by E. Kaldis (North-Holland, Amsterdam, 1978), pp. 603–656.
- ⁵R. Griessen and T. Riesterer, in *Hydrogen in Intermetallic Compounds I*, Vol. 63 of *Topics in Applied Physics*, edited by L. Schlapbach (Springer-Verlag, Berlin, 1988), pp. 219–284.
- ⁶J. K. Nørskov, Phys. Rev. B **26**, 2875 (1982).
- ⁷A. R. Williams, J. Kübler, and C. D. Gelatt, Phys. Rev. B **19**, 6094 (1979).
- ⁸R. Griessen, Phys. Rev. B **38**, 3690 (1988).
- ⁹M. Yoshihara and R. B. Mclellan, J. Phys. Chem. Solids **43**, 539 (1982).
- ¹⁰R. Kirchheim, Acta Metall. **30**, 1069 (1982).
- ¹¹M. Koiwa, Acta Metall. **22**, 1259 (1974).
- ¹²R. B. Mclellan and M. Yoshihara, Acta Metall. **35**, 197 (1987).
- ¹³R. Griessen, in *Hydrogen in Disordered and Amorphous Solids*, edited by G. Bambakidis and R. C. Bowman (Plenum, New York, 1986), pp. 153–172.
- ¹⁴R. Feenstra, R. Brouwer, and K. Griessen, Europhys. Lett. **7**, 425 (1988).
- ¹⁵R. C. Brouwer, E. Salomons, and R. Griessen, Phys. Rev. B **38**, 10217 (1988).
- ¹⁶M. Manninen, M. J. Puska, R. M. Nieminen and P. Jena, Phys. Rev. B **30**, 1065 (1984).
- ¹⁷A. I. Shirley and C. K. Hall, Acta Metall. **32**, 49 (1984).
- ¹⁸R. Griessen, Phys. Rev. B **27**, 7575 (1983).
- ¹⁹G. Boureau, J. Phys. Chem. Solids **42**, 743 (1981).
- ²⁰M. Cyrot and F. Cyrot-Lackmann, J. Phys. F **6**, 2257 (1976).
- ²¹R. Griessen and A. Driessen, Phys. Rev. B **30**, 4372 (1984).
- ²²S. Froyen and C. Herring, J. Appl. Phys. **52**, 7165 (1981).
- ²³W. Joss, R. Griessen and E. Fawcett, *Electron States and Fermi Surfaces of Homogeneously Strained Metallic Elements*, Vol. 12 of *Landolt-Börnstein, New Series, Metals: Phonon States, Electron States and Fermi Surfaces*, edited by K. H. Hellwege (Springer, Heidelberg, 1983), p. 1.
- ²⁴R. Feenstra, R. Griessen, and D. G. de Groot, J. Phys. F **16**, 1933 (1986).
- ²⁵R. Feenstra, P. Meuffels, B. Bischof, and H. Wenzl (unpublished).
- ²⁶D. T. Peterson and H. M. Herro, Metall. Trans. **18A**, 249 (1987).
- ²⁷D. T. Peterson and S. O. Nelson, Metall. Trans. **16A**, 367 (1985). The data obtained from this paper were recalculated leaving out the solubilities at 223 K. The data at this temperature were less precise than data obtained at higher temperatures and have all a systematic deviation, as can be seen in Fig. 10 of this reference.
- ²⁸J. F. Lynch, J. J. Reilly, and F. Millot, J. Phys. Chem. Solids **39**, 883 (1978).
- ²⁹J. F. Lynch, J. Phys. Chem. Solids **42**, 411 (1981).
- ³⁰Y. Saito and Y. Fukai, J. Less-Common Met. **138**, 161 (1988).
- ³¹R. Kirchheim, P. C. Camargo, and J. R. G. Da Silva, J. Less-Common Met. **95**, 293 (1983).
- ³²K. W. Katahara, M. H. Manghnani, and E. S. Fisher, J. Phys. F **9**, 773 (1979).
- ³³M. Mrowietz and A. Weiss, Ber. Bunsenges. Phys. Chem. **89**, 49 (1985).
- ³⁴V. L. Moruzzi, J. F. Janak, and A. R. Williams, in *Calculated Electronic Properties of Metals* (Pergamon, New York, 1978).
- ³⁵*Handbook of Chemistry and Physics*, 59th ed., edited by R. C. Weast and M. J. Astle (CRC, West Palm Beach, Florida, 1978), pp. E81–E83.
- ³⁶K. Gschneider, in *Solid State Physics*, edited by F. Seitz, D. Turnbull, and H. Ehrenreich (Academic, New York, 1964), Vol. 16, p. 275.
- ³⁷R. Griessen and R. Feenstra, J. Phys. F **15**, 1013 (1985).
- ³⁸E. S. Fischer, J. F. Miller, H. L. Alberts, and D. G. Westlake, J. Phys. F **11**, 1557 (1981).
- ³⁹R. C. Brouwer and R. Griessen, Phys. Rev. Lett. **62**, 1760 (1989).
- ⁴⁰J. M. Dupouy and B. L. Averbach, Acta Metall. **9**, 755 (1961).
- ⁴¹M. Mrowietz and A. Weiss, Ber. Bunsenges. Phys. Chem. **89**, 362 (1985).
- ⁴²S. Tanaka and H. Kimura, Trans. Jpn. Inst. Met. **20**, 647 (1979).
- ⁴³D. Nguyen Manh, D. Mayou, A. Pasturel, and F. Cyrot-Lackmann, J. Phys. F **15**, 1911 (1985).
- ⁴⁴R. Lässer, P. Meuffels, and R. Feenstra, in Kernforschungsanlage Jülich Report No. 2183, 1988 (unpublished).
- ⁴⁵D. G. Westlake and J. F. Miller, J. Less-Common Met. **65**, 139 (1979).
- ⁴⁶J. F. Lynch and J. Tanaka, Acta Metall. **29**, 537 (1981).
- ⁴⁷T. Eguchi and S. Morozumi, J. Jpn. Inst. Met. (Nippon Kinzoku Gakkaishi) **38**, 1019 (1974).
- ⁴⁸P. S. Rudman, Acta Metall. **12**, 1381 (1964).